DOI: 10.1002/ejic.201100249

Supramolecular Assemblies Directed by Hydrogen Bonds and π–π Interactions and Based on *N*-Heterocyclic-Ligand-Modified β-Octamolybdate – Structure and Catalytic Application in Olefin Epoxidation

Juan Du,[a,b] Jiehui Yu,[a] Jianyuan Tang,[a] Jing Wang,[a] Wenxiang Zhang,[a]
Werner R. Thiel,[c] and Mingjun Jia*[a]

Keywords: Supramolecular chemistry / *N*-Heterocyclic ligands / Polyoxometalates / Epoxidation / Heterogeneous catalysis

A series of supramolecular assemblies based on POMs modified by organic ligands, including $(Himi)_4[(imi)_2(Mo_8O_{26})]\cdot H_2O$ (**1**), $(H_2bbi)_2[Mo_8O_{26}]$ (**2**), and $(H_2bbi)[(Hbbi)_2(Mo_8O_{26})]\cdot H_2O$ (**3**), were synthesized by a one-step hydrothermal method. All of them are active catalysts for the epoxidation of olefins with *tert*-butyl hydroperoxide as the oxidant. Most interestingly, $(Himi)_4[(imi)_2(Mo_8O_{26})]\cdot H_2O$ (**1**) exhibits very high catalytic activity and stability, which makes it a truly efficient heterogeneous catalyst for olefin epoxidation.

Introduction

Polyoxometalates (POMs) are a unique class of metal oxide clusters. They show a series of unusual physicochemical properties, which make them attractive for applications in medicine, biology, materials science, and catalysis.[1] The use of POMs as epoxidation (or oxidation) catalysts turned out to be of special importance for applications due to their extraordinary ability to transfer oxygen atoms with high efficiency.[2] However, almost all sophisticated POMs or POM-based epoxidation catalysts are homogeneous in essence,[3] although heterogeneous catalysts would be more preferable with respect to a simple separation and recovery of the catalysts and their use in flow bed reactors.

Different approaches have been developed for the synthesis of heterogeneous POM-based catalysts. Probably the most popular way is to immobilize POMs on the surface of solid supports by either covalent or electrostatic binding.[4] However, in contrast to the immobilization of single-site metal catalysts, it is quite difficult to establish a stable linkage between the solid support and the POMs because of the large molecular size of the POM clusters. Undesirable dissolving or leaching of the active POM species during the oxidation reaction is a common problem for heterogeneous POM-based catalysts. It is therefore still an attractive and challenging effort to design highly efficient and environmentally benign heterogeneous POM-based epoxidation or oxidation catalysts.

Recently, a new class of ligand-modified POMs bearing multidimensional supramolecular structures have been synthesized by self-assembly of organic ligands and POMs.[5] The dynamic structures and the chemical properties of these new materials can be adjusted over a wide range by changing the types of the POMs, the ligands, or the linking methods, and/or by introduction of other transition metals.[6] Although these materials have fascinating structures and highly interesting physical and chemical properties, the investigation of their performance in heterogeneous olefin epoxidation is still rather rare.

Molybdenum compounds are well established catalysts for oxygen transfer reactions in biological systems and in industry.[7] Oxides, peroxides, and other types of molybdenum complexes have already been used for the development of heterogeneous epoxidation catalysts.[8] In this paper, we present a series of *N*-heterocyclic ligands used to modify β-octamolybdate-based POMs for the synthesis of heterogeneous olefin epoxidation catalysts. These materials, which are accessible by a one-step hydrothermal method, include $(Himi)_4[(imi)_2(Mo_8O_{26})]\cdot H_2O$ (**1**), $(H_2bbi)_2[Mo_8O_{26}]$ (**2**) {H_2bbi = 1,1′-(1,4-butanediyl)bis(imidazolium)}, and (H_2bbi) $[(Hbbi)_2(Mo_8O_{26})]\cdot H_2O$ (**3**). We found that all these compounds possess supramolecular structures, which are self-assembled by linking the octamolybdate clusters with imidazolium cations and water molecules through hydrogen bonds and π–π interactions. Most interestingly, compound **1** exhibits very high catalytic activity in the epoxidation of olefins (including terminal 1-octene) with *tert*-butyl hydroperoxide (*t*BuOOH) as the oxidant; it is also stable against

---

[a] State Key Laboratory of Theoretical and Computational Chemistry, College of Chemistry, Jilin University,
130021 Changchun, China
Fax: +86-43185168420
E-mail: jiamj@jlu.edu.cn
[b] College of Chemistry, Jilin Normal University,
136000 Siping, China
[c] Technische Universität Kaiserslautern, Fachbereich Chemie,
Erwin-Schrödinger-Str., Geb. 54, 67663 Kaiserslautern,
Germany
Fax: +49-631-205-4676

Supporting information for this article is available on the WWW under http://dx.doi.org/10.1002/ejic.201100249.

leaching. Thus, it is a truly efficient heterogeneous catalyst for this reaction.

Results and Discussion

The crystal structure of **1** shows the presence of a discrete octamolybdate cluster[5c] modified by two imidazole moieties, four imidazolium cations, and one uncoordinated water molecule (Figure S1). The imidazole ligands coordinate to the $\{Mo_8O_{26}\}^{4-}$ unit by one of their nitrogen atoms. Catalyst **1** appears to be similar to one reported in the literature,[9] although the synthesis was carried out under different conditions.

We found that catalyst **1** also possesses 3D supramolecular structure based on the unit $[(imi)_2(Mo_8O_{26})]^{4-}$ and the four imidazolium cations, which are connected through strong H-bond interactions of the type N–H···O (Figures S2–S4). Each uncoordinated water molecule connects to the adjacent cluster through a hydrogen bond of the type O–H···O (Figure S5).

Apart from these, π–π interactions dominate the crystal packing (Figure 1), through which three adjacent imidazolium cations comprise a group. The centroid–centroid distances of the alternatively parallel imidazole rings are 3.46 Å and 3.50 Å (Figure 1b). In addition, these imidazolium cations link O atoms of adjacent $[(imi)_2(Mo_8O_{26})]^{4-}$ clusters through more than one hydrogen bond of the type N–H···O (Figure S6). Undoubtedly, both the hydrogen bonds and π–π interactions should play important roles in the supramolecular structure of catalyst **1**.[10]

The unit cell of **2** contains a $[Mo_8O_{28}]^{8-}$ octamolybdate anion[5c] and two $[H_2bbi]^{2+}$ cations (Figure S7). The structure of catalyst **2** contains infinite anionic molybdenum oxide chains, which are built of the octamolybdate units repeated by translation and connected by pairs of common vertices (Figure S8). The organic cations H_2bbi adopt two different conformations. The two types of H_2bbis link the adjacent 1D molybdenum oxide chains trough hydrogen bonds to form two kinds of 2D supramolecular layer in different directions (Figure S9), and the two kinds of 2D supramolecular framework combine to form the 3D supramolecular framework of catalyst **2** (Figure 2). Catalyst **2** appears to be similar to one reported in the literature,[11] although the synthesis was carried out under different conditions.

The molecular structure of catalyst **3** consists of one $[(Hbbi)_2(Mo_8O_{26})]^{2-}$ unit, one $(H_2bbi)^{2+}$ cation, and one water molecule (Figure 3). The $(Hbbi)^+$ fragment coordinates to the $\{Mo_8O_{26}\}^{4-}$ unit by one of its nitrogen atoms. Each $[(Hbbi)_2(Mo_8O_{26})]^{2-}$ cluster is connected to two adjacent clusters by N–H···O hydrogen bonds between the nitrogen atoms of the two coordinated $(Hbbi)^+$ units and two oxygen atoms of neighboring POMs leading to a 1D supramolecular chain (Figure 4).

The 1D supramolecular chains are alternately arranged on the same or on different layers (Figure S10). The $(H_2bbi)^{2+}$ cations are inserted vertically in the cavities between adjacent 1D supramolecular chains (Figure S10a). Every uncoordinated water molecule is connected to an O

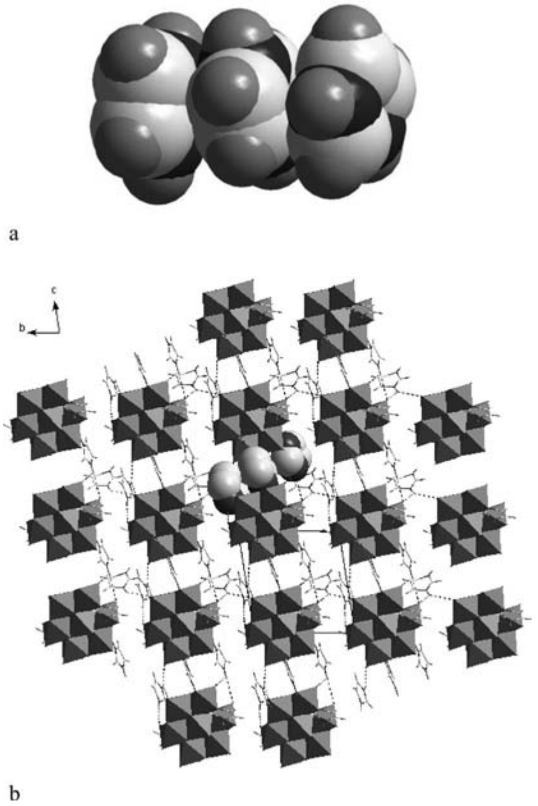

Figure 1. Packing in the unit cell of **1** dominated by π–π stacking interactions (Å, dotted lines) between imidazolium cations.

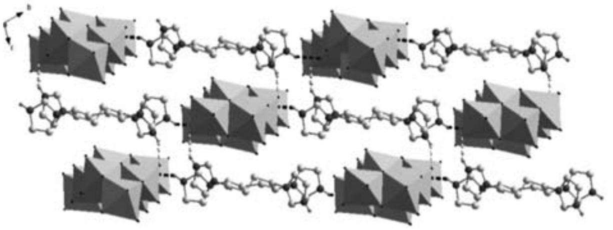

Figure 2. The 3D supramolecular network of **2** formed by two types of H_2bbi ligands and adjacent molybdenum oxide chains via N–H···O hydrogen bonds.

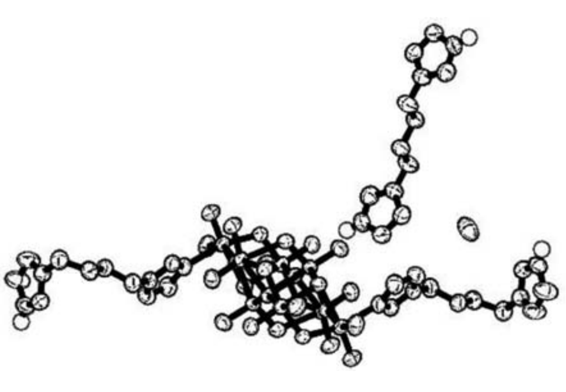

Figure 3. Molecular unit structure of catalyst **3** in the solid state.

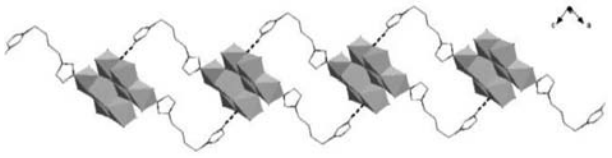

Figure 4. A polyhedral representation of the 1D supramolecular chain in **3**, built of $[(Hbbi)_2(Mo_8O_{26})]$ clusters linked through hydrogen bonds (dotted lines represent hydrogen bonds).

atom of adjacent clusters through O–H···O hydrogen bonds (Figure S11).

The catalytic epoxidation performances of **1**–**3** were first investigated for cyclooctene with *t*BuOOH as the oxidant. As shown in Table 1, all the catalysts are active with nearly 100% selectivity for epoxycyclooctene. Among them, catalyst **1** shows the highest epoxidation activity, and a 96.6% conversion of cyclooctene could be achieved after 12 h reaction at a temperature of 35 °C.

Table 1. Activities of the three catalysts in the epoxidation of *cis*-cyclooctene.[a]

Entry	Catalysts	Temperature (°C)	Time (h)	Conversion (%)
1	**1**	35	3	48.9
			6	82.0
			12	96.6
2	**1**	45	3	62.3
			6	88.5
			12	99.2
3	**2**	45	3	36.4
			6	63.5
			12	92.9
4	**3**	45	3	38.1
			6	60.0
			12	86.6

[a] Reaction conditions: catalyst 0.006 mmol; *cis*-cyclooctene 1.0 mmol; *tert*-butylhydroperoxide 1.0 mmol; chloroform 2 mL. All selectivities for the epoxide are greater than 99%.

Additional experiments proved that catalyst **1** has excellent stability against leaching of active species under the reaction conditions employed, while a slight leaching of the active species was observed for catalysts **2** and **3**.

The reusability of catalyst **1** was also evaluated. This catalyst could be recycled at least five times without obvious loss of activity or selectivity under identical reaction conditions. In the duplicate reaction, there was almost no detectable subsequent conversion in the filtrate after removal of **1**. In contrast, the conversion of cyclooctene proceeded at a very low rate in the solution remaining after removing catalysts **2** and **3** by filtration at the reaction temperature. This means that almost no active species were leached from **1** under the reaction conditions (Figure S12). This is very strong evidence that **1** is a really heterogeneous catalyst.

Furthermore, the catalytic activity and reusability of catalyst **1** were investigated for the epoxidation of 1-octene with *tert*-butylhydroperoxide at 61 °C (Figure 5). Clearly, this catalyst is quite active for the epoxidation of 1-octene, nearly 100% conversion of 1-octene could be obtained after 6 h. In addition, this catalyst could also be successfully recycled at least four times without losing activity, and no detectable leaching of the active species could be observed during the course of the reaction, which indicates the truly heterogeneous nature of this catalyst.

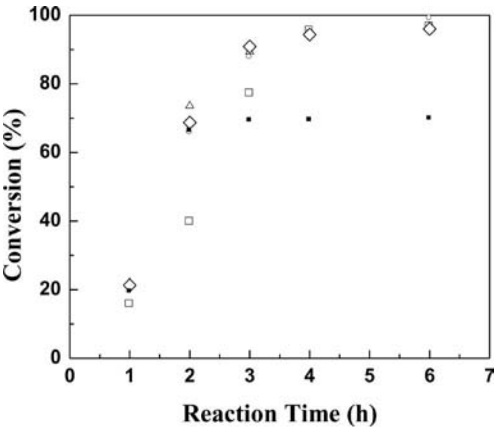

Figure 5. Epoxidation of 1-octene at 61 °C with catalyst **1**: Run 1 with fresh catalyst, subsequent runs with recovered catalyst [run 1 (□), run 2 (○), run 3 (Δ), run 4 (◇), the catalyst was removed after 2 h (■)].

By comparing the IR and XRD spectra (Figures S13 and S14, respectively) of catalyst **1** before and after the reactions, it was found that there were almost no obvious differences. Furthermore, the elemental analysis results of the recycled sample of **1** are consistent with those of the fresh sample before reaction. These results provide additional evidences that catalyst **1** is extremely stable under the given reaction conditions.

The fact that catalyst **1** shows much higher catalytic activity might be mainly attributed to the presence of coordinated imidazole ligands in this compound. Structural analyses have shown that the $(Mo_8O_{26})^{4-}$ units in the primary structure of **1** have two bound imidazole ligands. Here the imidazole ring connects to a Mo atom of $[Mo_8O_{26}]^{4-}$ to form a conjugative π bond with five centers of six electrons. Such an influence may enhance the electropositivity of Mo species, thus resulting in the improvement of its ability to attract or capture nucleophilic groups, which leads to the improvement of the epoxidation activity of the catalyst. Moreover, the special supramolecular structure of **1**, which is formed by self-assembly of the anions and cations through *extensive* hydrogen bonding and π–π interaction, may play an important role in improving the stability of the POM-based catalyst.

Conclusions

Supramolecular assemblies based on *N*-heterocyclic-ligand-modified β-octamolybdate were found to be truly efficient heterogeneous catalysts for olefin epoxidation. The formation of multidimensional supramolecular structure through multiple weak interactions, such as hydrogen bonds and π–π interactions, should be a critical factor in preparing active and stable POM-based catalysts.

Experimental Section

General: MoO_3 (≥ 99.5%), H_2MoO_4 (85.0–90.0%), $(NH_4)_6Mo_7O_{24}\cdot 4H_2O$ (≥ 99%), imidazole (imi, ≥ 99%), nicotinic acid (nic, ≥ 99.5%), *cis*-cyclooctene (95%), 1-octene (95%), *tert*-butylhydroperoxide (TBHP, 5.0–6.0 M solution in decane, containing less than 4% water), chloroform (≥ 99%) were obtained commercially and used without additional purification. IR spectra were recorded in the range 350–4000 cm^{-1} with a Nicolet Impact 410 FTIR spectrometer by using KBr pellets. Thermal gravimetric (TG) analyses were performed with a Perkin–Elmer TGA7 instrument in flowing N_2 with a heating rate of 10 °C min^{-1}. Powder X-ray diffraction (XRD) measurements were performed with a Shimadzu XRD-6000 diffractometer (40 kV, 30 mA) by using Ni-filtered Cu-K_α radiation in the angular range 2θ = 5–70° at 293 K.

Catalyst Tests: Each catalytic test was performed in a sealed round-bottomed flask with vigorous stirring at 35–61 °C for a given period of time. Typically, the epoxidation reaction was initiated by adding *tert*-butylhydroperoxide (1.0 mmol) to a mixture containing the olefin (1.0 mmol), the catalyst (0.006 mmol), and chloroform (2 mL). Samples were withdrawn periodically and filtered before being analyzing with a Shimadzu GC-8A. The performance of the catalyst was evaluated quantitatively by the conversion of the reactants.

1,1′-(1,4-Butanediyl)bis(imidazole) (bbi):[12] A mixture of imidazole (3.4 g, 50 mmol) and NaOH (2.0 g, 50 mmol) in DMSO (10 mL) was stirred at 60 °C for 1 h. Then 1,4-dichlorobutane (3.2 g, 25 mmol) was added. The mixture was cooled to room temperature after being stirred at 60 °C for 2 h; it was then poured into water (200 mL). A white solid formed almost immediately, which was filtered off, washed with water, and dried in air. Yield: 4.1 g.

1: MoO_3 (0.2159 g, 1.5 mmol), H_2MoO_4 (0.2429 g, 1.5 mmol), imidazole (0.1634 g, 2.4 mmol), and water (15 mL) were added to a flask in succession. NaOH solution (1 M) was used to adjust the pH to 7, and the mixture was continuously stirred for 1 h at room temperature. The turbid mixture was sealed in a 25 mL Teflon-lined autoclave and heated to 140 °C for 96 h, followed by cooling to room temperature at a rate of 10 °C h^{-1}. Light blue block crystals, suitable for X-ray analysis, were obtained. The entire yield, based on Mo, is 68% . IR (KBr): 1641 (m), 1588 (s), 1543 (m), 1497 (m), 1416 (m), 1325 (m), 1265 (m), 1182 (m), 1144 (m), 1091 (m), 1077 (s), 1054 (s), 933 (s), 906 (s), 836 (s), 755 (s), 657 (s), 627 (s), 553 (s), 523 (s), 483 (s), 442 (m). $(C_3H_5N_2)_4[(C_3N_2H_4)_2(Mo_8O_{26})]\cdot H_2O$ (1614.06): calcd. C 13.39, H 1.87, Mo 47.56, N 10.42; found C 13.49, H 1.96, Mo 47.72, N 10.29.

2: $(NH_4)_6Mo_7O_{24}\cdot 4H_2O$ (0.124 g, 0.1 mmol), bbi (0.038 g, 0.2 mmol), and water (15 mL) were added to a flask in succession. Diluted hydrochloric acid was used to adjust the pH to 4.5. The mixture was stirred for 1 h at room temperature and then sealed in a 25 mL Teflon-lined autoclave and heated at 170 °C for 120 h, followed by cooling to room temperature at a rate of 10 °C h^{-1}. Block type, light green crystals were obtained (yield ca. 66% based on Mo). IR (KBr): 3098 (s), 1575 (s), 1533 (s), 1435 (s), 1400 (s), 1303 (s), 1085 (s), 946 (s), 875 (s), 820 (s), 757 (s), 603 (s), 477 (m). $(C_5H_8N_2)_2(Mo_4O_{13})$ (784.03): calcd. C 15.32, H 2.05, Mo 48.95, N 7.15; found C 15.21, H 2.13, Mo 48.80, N 7.02.

3: $(NH_4)_6Mo_7O_{24}\cdot 4H_2O$ (0.124 g, 0.1 mmol), bbi (0.038 g, 0.2 mmol), and water (15 mL) were added to a flask in succession. The mixture (pH = 6) was stirred for 1 h at room temperature and then sealed in a 25 mL Teflon-lined autoclave and heated at 170 °C for 120 h, followed by cooling to room temperature at a rate of 6 °C h^{-1}. Light green block type crystals, suitable for X-ray analysis, were collected. The entire yield based on Mo is 73%. IR (KBr): 3107 (s), 1637 (m), 1581 (m), 1524 (m), 1464 (m), 1441 (m), 1412 (m), 1385 (m), 1344 (m), 1304 (m), 1281 (m), 1240 (m), 1176 (m), 1109 (s), 1086 (s), 1032 (s), 1012 (m), 935 (s), 901 (s), 872 (s), 837 (s), 764 (s), 687 (s), 631 (s), 592 (s), 519 (s), 476 (s), 418 (m). $(C_{10}H_{16}N_4)[(C_{10}N_4H_{15})_2(Mo_8O_{26})]\cdot H_2O$ (1776.32): calcd. C 20.63, H 1.04, Mo 43.96, N 9.63, O 26.76; found C 20.57, H 1.12, Mo 43.92, N 9.89, O 26.54.

Crystallographic Details

Intensity data were measured with a Siemens SMART CCD having graphite-monochromatized Mo-K_α radiation (λ = 0.71073 Å) at 293 K and corrected for absorption by the SADABS program.[13] The structures were solved by direct methods and refined by the full-matrix least-squares method with the SHELXL-97 program package.[14] The hydrogen atoms attached to carbon positions were placed in geometrically calculated positions.

Compound 3: $C_{30}H_{50}Mo_8N_{12}O_{28}$, M_r = 1794.34, light blue block crystals, triclinic, space group $P\bar{1}$, a = 11.3376(1) Å, b = 11.8248(1) Å, c = 12.1607(2) Å, α = 60.9280(1)°, β = 70.254(2)°, γ = 65.5030(1)°, V = 1277.4(2) $Å^3$, Z = 2, $\rho_{calcd.}$ = 2.332 g cm^{-3}, T = 296 K, μ = 1.998 mm^{-1}, 9452 reflections collected, 6306 independent reflections (R_{int} = 0.0167), 6306 reflections observed [$I > 2\sigma(I)$], 360 refined parameters, final R indices [$I > 2\sigma(I)$]: R_1 = 0.0282, wR_2 = 0.0718, R indices (all data): R_1 = 0.0323, wR_2 = 0.0750.

CCDC-806737 (for **3**) contains the supplementary crystallographic data for this paper. These data can be obtained free of charge from The Cambridge Crystallographic Data Centre via www.ccdc.cam.ac.uk/data_request/cif.

Supporting Information (see footnote on the first page of this article): Details of the molecular structures and supramolecular frameworks of compounds **1** to **3**, the heterogeneous reaction check for **1**–**3**, and the XRD and IR spectra of compound **1** before and after the reactions.

Acknowledgments

Financial support from the National Natural Science Foundation of China and Jilin University (20403006, 20773050) is gratefully acknowledged.

---

[1] a) T. Okuhara, *Chem. Rev.* **2002**, *102*, 3641–3666; b) G. Grigoropoulou, J. H. Clark, J. A. Elings, *Green Chem.* **2003**, *5*, 1.

[2] D. L. Long, R. Tsunashima, L. Cronin, *Angew. Chem.* **2010**, *122*, 1780–1803.

[3] a) T. Okuhara, N. Mizuno, M. Misono, *Appl. Catal. A: General* **2001**, *222*, 63–77; b) I. V. Kozhevnikov, *Chem. Rev.* **1998**, *98*, 171–198.

[4] a) N. V. Maksimchuk, K. A. Kovalenko, S. S. Arzumanov, Y. A. Chesalov, M. S. Melgunov, A. G. Stepanov, V. P. Fedin, O. A. Kholdeeva, *Inorg. Chem.* **2010**, *49*, 2920–2930; b) J. Kasai, Y. Nakagawa, S. Uchida, K. Yamaguchi, N. Mizuno, *Chem. Eur. J.* **2006**, *12*, 4176–4184; c) W. Qi, Y. Z. Wang, W. Li, L. X. Wu, *Chem. Eur. J.* **2010**, *16*, 1068–1078; d) P. Liu, C. H. Wang, C. Li, *J. Catal.* **2009**, *262*, 159–168.

[5] a) Z. G. Han, T. Chai, Y. N. Wang, Y. Z. Gao, C. W. Hu, *Polyhedron* **2010**, *29*, 196–203; b) X. He, J. W. Ye, J. N. Xu, Y. Fan, L. Wang, P. Zhang, Y. Wang, *J. Mol. Struct.* **2005**, *749*, 9–12; c) K. Pavani, S. E. Lofland, K. V. Ramanujachary, A. Ramanan, *Eur. J. Inorg. Chem.* **2007**, 568–578; d) Z. Han, Y. Z. Gao, X. L. Zhai, J. Peng, A. X. Tian, Y. L. Zhao, C. W. Hu, *Cryst. Growth Des.* **2009**, *9*, 1225–1234.

[6] a) Y. P. Ren, X. J. Kong, X. Y. Hu, M. Sun, L. S. Long, R. B. Huang, L. S. Zheng, *Inorg. Chem.* **2006**, *45*, 4016–4023; b) J. Q. Sha, J. Peng, H. S. Liu, J. Chen, B. X. Dong, A. X. Tian, Z. M. Su, *Eur. J. Inorg. Chem.* **2007**, 1268–1274; c) L. M. Rodriguez-Albelo, A. R. Ruiz-Salvador, A. Sampieri, D. W. Lewis, A. Gómez, B. Nohra, P. Mialane, J. Marrot, F. Sécheresse, C. Mellot-Draznieks, R. Ngo Biboum, B. Keita, L. Nadjo, A. Dolbecq, *J. Am. Chem. Soc.* **2009**, *131*, 16078–16087.

[7] a) G. P. Chisole, P. M. Maitlis, *Metal Catalysis in Industrial Organic Processes*, Royal Society of Chemistry Publishing, Cambridge, U. K., **2008**; b) R. Hille, *Trends Biochem. Sci.* **2002**, *27*, 360–367.

[8] a) M. V. Dias, C. D. Nunes, P. D. Vaz, P. Ferreira, P. Brandão, V. Félix, M. J. Calhorda, *J. Catal.* **2008**, *256*, 301–311; b) K. Ambroziak, R. Mbeleck, Y. He, B. Saha, D. C. Sherrington, *Ind. Eng. Chem. Res.* **2009**, *48*, 3293–3302; c) M. J. Jia, W. R. Thiel, *Chem. Commun.* **2002**, 2392–2393; d) M. J. Jia, A. Seifert, W. R. Thiel, *J. Catal.* **2004**, *221*, 319–324; e) M. Abrantes, T. R. Amarante, M. M. Antunes, S. Gago, F. A. A. Paz, I. Margiolaki, A. E. Rodrigues, M. Pillinger, A. A. Valente, I. S. Gonçalves, *Inorg. Chem.* **2010**, *49*, 6865–6873; f) S. Shylesh, M. J. Jia, W. R. Thiel, *Eur. J. Inorg. Chem.* **2010**, 4395–4410.

[9] C. B. Li, Z. G. Zong, J. Gong, S. W. Ng, *Acta Crystallogr., Sect. E: Struct. Rep. Online* **2007**, *63*, 2320.

[10] a) M. J. Krische, J. M. Lehn, *Struct. Bonding (Berlin)* **2000**, *96*, 3–29; b) R. Cao, S. X. Liu, L. H. Xie, Y. B. Pan, J. F. Cao, Y. H. Ren, L. Xu, *Inorg. Chem.* **2007**, *46*, 3541–3547.

[11] X. L. Wang, B. K. Chen, G. C. Liu, H. Y. Zhao, H. Y. Lin, H. L. Hu, *Solid State Sci.* **2009**, *11*, 61–67.

[12] J. F. Ma, J. F. Liu, Y. Xing, H. Q. Jia, Y. H. Lin, *J. Chem. Soc., Dalton Trans.* **2000**, 2403–2407.

[13] G. M. Sheldrick, *SADABS: Siemens Analytical X-ray Instrument Division*, Madison, WI, **1995**.

[14] G. M. Sheldrick, *SHELXL-97: A Program for Crystal Structure Determination*, University of Göttingen, Germany, **1997**.

Received: March 13, 2011